Genes Genet. Syst. (2014) **89**, p. 121–131

QTL analysis of genetic loci affecting domestication-related spike characters in common wheat

Mazen Katkout[1], Masahiro Kishii[2], Kanako Kawaura[1], Kouhei Mishina[1], Shun Sakuma[1], Kazuko Umeda[1], Shigeo Takumi[3], Miyuki Nitta[4], Shuhei Nasuda[4] and Yasunari Ogihara[1]*

[1]*Kihara Institute for Biological Research and Department of Life and Environmental System Science, Graduate School of Nanobioscience, Yokohama City University, Maioka-cho 641-12, Totsuka-ku, Yokohama 244-0813, Japan*
[2]*International Maize and Wheat Improvement Center (CIMMYT), Km. 45, Carretera, Mexico-Veracruz El Batan, Texcoco CP56237, Edo. De Mexico, Mexico*
[3]*Laboratory of Plant Genetics, Graduate School of Agricultural Science, Kobe University, Rokkodai-cho 1-1, Nada-ku, Kobe 657-8501, Japan*
[4]*Laboratory of Plant Genetics, Graduate School of Agriculture, Kyoto University, Kitashirakawaoiwake-cho, Sakyo-ku, Kyoto 606-8502, Japan*

(Received 23 July 2014, accepted 17 September 2014)

Domestication-related changes that govern a spike morphology suitable for seed harvesting in cereals have resulted from mutation and selection of the genes. A synthetic hexaploid wheat (S-6214, genome AABBDD) produced by a cross between durum wheat (AABB) and wild goat grass (DD) showed partial non-domestication-related phenotypes due to genetic effects of the wild goat grass genome. Quantitative trait loci (QTLs) affecting wheat domestication-related spike characters including spike threshability, rachis fragility and spike compactness were investigated in F_2 progeny of a cross between Chinese Spring (CS) wheat (AABBDD) and S-6214. Of 15 relevant QTLs identified, eight seemed to be consistent with peaks previously reported in wheat, while four QTL regions were novel. Four QTLs that affected spike threshability were localized to chromosomes 2BS, 2DS, 4D and 5DS. The QTL on 2DS probably represents the tenacious glume gene, *Tg-D1*. Based on its map position, the QTL located on 2BS coincides with *Ppd-B1* and seems to be a homoeolocus of the soft glume gene. Two novel QTLs were detected on 4D and 5DS, and their goat grass alleles increased glume tenacity. Three novel QTLs located on 2DL, 3DL and 4D for rachis fragility were found. Based on the map position, the QTL on 3DL seems different from *Br1* and *Br2* loci and its CS allele appears to promote the generation of barrel-type diaspores. Three disarticulation types of spikelets were found in F_2 individuals: wedge-type, barrel-type and both types. Among eight QTL peaks that governed spike morphology, six, located on 2AS, 2BS, 2DS, 4AL and 5AL, coincided with ones previously reported. A QTL for spike compactness on 5AL was distinct from the *Q* gene. A novel QTL that controls spike length was detected on 5DL. Complex genetic interactions between genetic background and the action of each gene were suggested.

Key words: QTL mapping, rachis fragility, threshability, spike morphology, wheat domestication

INTRODUCTION

Common wheat (*Triticum aestivum* L., AABBDD genome, 2n = 6x = 42) evolved by hybridization between cultivated emmer wheat (*T. turgidum* ssp. *dicoccum* L., AABB genome, 2n = 4x = 28) and goat grass (*Aegilops tauschii* Coss., DD, 2n = 2x = 14) (Kihara, 1944; McFadden and Sears, 1946). For successful cultivation of hexaploid wheat, suppression of wild characters from goat grass and improvement of agronomical traits in the amphiploid were important. Target traits for domestication might include morphological ones related to seed dispersal such as rachis fragility, spike disarticulation, glume tenacity

Edited by Yoshihiko Tsumura
* Corresponding author. E-mail: yogihara@yokohama-cu.ac.jp

and threshability. Modern cultivated durum wheat (*T. turgidum* ssp. *durum*, AABB, 2n = 4x = 28) and common wheat exhibit highly domesticated characters (Li and Gill, 2006).

The *Q* gene in wheat encodes an APETALA2-like transcription factor that mainly confers square-headedness (short compact spike) and pleiotropically affects rachis fragility and glume tenacity, which are responsible for free-threshability (Muramatsu, 1963; Simons et al., 2006). *T. aestivum* cv. Chinese Spring (CS, AABBDD) and *T. turgidum* ssp. *durum* cv. Langdon (LDN, AABB) have an identical *Q* gene at the nucleotide level of the coding sequences in the gene (Simons et al., 2006; Abdollahi et al., 2012).

Another genetic factor controlling threshability resides in the D genome of synthetic hexaploid wheat (AABBDD) that was produced between a free-threshing tetraploid (AABB) and wild goat grass (DD) (Kerber and Dyck, 1969). A synthetic wheat was non-free-threshing, even though it inherited the *Q* gene. The gene responsible was later identified as a partially dominant gene, *Tg1* (*tenacious glumes 1*; renamed by Li and Gill (2006) and referred to hereafter as *Tg-D1*), and mapped on the short arm of chromosome 2D (2DS) (Kerber and Rowland, 1974; Simonetti et al., 1999; Jantasuriyarat et al., 2004; Nalam et al., 2006; Sood et al., 2009; Dvorak et al., 2012). *Tg-D1* inhibits the action of *Q*.

Modern durum wheat and common wheat have a tough rachis governed by the gene *br* (*brittle rachis*). On the other hand, wild and semi-wild types of *Triticum* and *Aegilops* species harbor dominant genes (*Br*) that govern rachis brittleness. The *Br* genes map to the homeologous group 3 chromosomes in *Triticum* and *Aegilops* species (Joppa and Cantrell, 1990; Chen et al., 1998; Watanabe et al., 2002, 2006; Li and Gill, 2006). Besides the brittleness type, rachis disarticulation can be divided into two types, wedge- and barrel-shaped, depending on the breakage point of spikelets. In wedge-type disarticulation, the breakage occurs on the upper side of the junction of the rachis and spikelet base. The associated rachis fragment remains attached below each spikelet (Fig. 1F, left). Wedge-type disarticulation is observed in species containing the A, B, G, S and T genomes (Kimber and Feldman, 1987), although some accessions of *Ae. speltoides* (SS) exhibit barrel-type disarticulation (Chen, 2001). In barrel-type disarticulation, the rachis fractures on the lower side of the junction between the rachis and spikelet base, leaving the adjacent fragment attached behind each spikelet (Fig. 1F, right). Barrel-type disarticulation occurs in species with the D genome. In the progeny of crosses of hexaploids between Tibetan semi-wild wheat and Yunnan hulled wheat, individuals having three disarticulation types (wedge-type, barrel-type and both) were found, even though each parental strain carries the *Q* gene and shows wedge-type disarticulation (Chen, 2001).

In addition to these effects of major genes, QTLs affecting spike threshability have also been reported on 2AS, 2BL, 5AS, 6AS and 6DL (Simonetti et al., 1999; Jantasuriyarat et al., 2004), and rachis fragility on 2BL and 7BL (Jantasuriyarat et al., 2004).

To better understand domestication-related spike traits in cultivated wheat, we produced a synthetic hexaploid wheat (S-6214) by crossing LDN with *Ae. tauschii* ssp. *strangulata* (KU-2097, DD). Since KU-2097 exhibits a fragile rachis, barrel-type disarticulation and a tenacious glume, its genotype should be *qqBrBrTgTg*. S-6214 shows a partially fragile rachis, wedge-type disarticulation and a tenacious glume. The F_2 population after a cross between CS wheat (*QQbrbrtgtg*, Li and Gill, 2006) and S-6214 (*QQBrBrTgTg*), where the *Q* genes from CS and LDN have identical coding sequences, was investigated to find novel QTLs that regulate domestication-related spike characters.

MATERIALS AND METHODS

Plant materials A synthetic wheat, S-6214, was produced by crossing LDN with KU-2097 at Kobe University, Japan. An F_2 mapping population was developed from a cross between CS and S-6214. The F_2 population and $F_{2:3}$ families along with their parents were grown under field conditions at the Kihara Institute for Biological Research, Yokohama City University; the phenotype of F_2 individuals was checked in 2010/2011 and that of F_3 individuals in 2011/2012.

Phenotyping Three randomly chosen main spikes were used for phenotypic evaluation. Spike length (SPL) was measured from the base of the rachis to the tip of the uppermost spikelet, excluding the awns. Spike compactness (CPT) was calculated by dividing the number of spikelets per spike (SPN) by spike length. To estimate free-threshability (FT), a single spike thresher (MR-D720; Twinbird, Sanjo, Japan) was used at its minimum power (1) and for a fixed time (5 sec) to liberate the grains of CS completely from the spike. Threshability was then measured as the percentage of threshed seeds from the total number of seeds per spike. Rachis fragility (RCH) was measured after threshing as the percentage of broken nodes to the total number of spike rachis nodes. The type of rachis disarticulation generated after mechanical threshing was scored as wedge-type, barrel-type or both. This classification was also applied for $F_{2:3}$ families. Pearson's correlation coefficients were calculated to determine the phenotypic correlation among traits.

DNA extraction and PCR DNA was extracted from 1 g leaf tissue from F_2 plants and parental lines as described previously (Saghai-Maroof et al., 1984). Polymerase chain

Fig. 1. The spike and its threshing in parents and progeny. (A) Spike of *Triticum turgidum* ssp. *durum* cv. Langdon (AABB). (B) Spike of *Ae. tauschii* ssp. *strangulata* (DD) with its barrel-type diaspores. (C) Spike of the synthetic wheat S-6214 (AABBDD). (D) Spike of *T. aestivum* cv. Chinese Spring. (E) Complete (100%) threshability of a Chinese Spring spike along with its intact rachis after threshing. (F) The three disarticulation types shown in progeny (F_2 plants and $F_{2:3}$ families): wedge-type (left), barrel-type (right), and a special type produced by spike rachises showing both types (middle). (G) Partial (~60%) threshability of S-6214 and (H) its wedge-type disarticulation after threshing. Scale bars, 1 cm.

reaction (PCR) amplification was performed in a 10-μl reaction containing 10 ng genomic DNA, 2 pmol each primer, 2 μl betaine (5 M) and 1x SapphireAmp fast PCR master mixture (Takara Bio, Otsu, Japan). PCR conditions were a denaturation step (94°C for 1 min), followed by 40 cycles of 98°C for 5 sec, 50–58°C (primer-dependent) for 5 sec and 72°C for 10 sec, with a final incubation at 72°C for 3 min, using a TP600 thermal cycler (Takara Bio). Amplicons were electrophoresed through 13% polyacrylamide gel, and were visualized by ethidium bromide staining.

Screening of SSR markers and development of a marker at the *Q* locus between CS and LDN A total of 342 published simple sequence repeat (SSR) markers (Roeder et al., 1998; Pestsova et al., 2000; Gupta et al., 2002; Guyomarc'h et al., 2002; Somers et al., 2004; Sourdille et al., 2004; Song et al., 2005) were used for screening. To develop a PCR-based marker to detect polymorphism at the *Q* locus between CS and LDN, BAC sequences spanning the *Q* locus from CS (acc. JF701619) and LDN (acc. JF701620) (Zhang et al., 2011) were aligned using CLC sequence viewer version 6.6.2 (Supplementary Fig. S1). We found a 16-bp insertion/deletion located 1568 bp upstream of the *Q* translation initiation site and designed primers (5´-GTACCTGCTCCGCCTGTG-3´ and 5´-CCCTCCCTCCCTCTAATCAA-3´) with an expected amplification product size of 180 bp in LDN and 164 bp in CS (Supplementary Fig. S2).

Genetic mapping Linkage maps were constructed with MAPMAKER/EXP version 3.0 (Lander et al., 1987). Recombination frequency was converted to genetic distance using the Kosambi mapping function (Kosambi, 1943). A framework map for each chromosome was constructed at a LOD score of 3.0, and the 'TRY' and 'RIPPLE' commands were then used to add markers to the framework map and check the final marker order, respectively, with 'DETECTION ERROR ON' to check for any putative misgenotyping. Markers were ordered at a minimum LOD score of 3.0 with the exception of co-segregating or closely linked markers. QTL mapping was performed by composite interval mapping (Zeng, 1993, 1994) using QTL Cartographer version 2.5 software (Wang et al., 2005). A forward-selection backward-elimination stepwise regression procedure was used to identify co-factors for composite interval mapping. A 10-cM scan window was used for all analyses, and the likelihood ratio statistic was computed every 2 cM. A genome-wide LOD threshold of 3.00 was used based on 1,000 permutations ($P < 0.05$). In a few cases, QTL peaks with a LOD score lower than 3.00 but higher than 2.50 were considered if supported by an overlapping QTL for a relevant trait or by previous genetic knowledge. Co-segregation of SSR alleles with disarticulation types and segregation ratios of all SSR loci were examined using a χ^2-test ($P < 0.05$). Due to the limited number of F_2 plants showing disarticulated diaspores, especially the barrel type, a larger population size (191 F_2 individuals) was used to test co-segregation with SSR alleles associated with rachis fragility after threshing. QTL peaks linked to significantly distorted marker loci were not considered. Linkage maps were drawn using MapChart 2.2 software (Voorrips, 2002).

RESULTS

Phenotypic evaluation Phenotypic traits of FT, RCH, SPL, SPN, and CPT were evaluated for CS, S-6214 and 117 individuals of their F_2 progeny (Table 1). The parental lines differed significantly in all traits studied (Table 1). CS had significantly higher spike density than S-6214. CS spikes had round soft glumes loosely enclosing the seeds, while those of S-6214 had keeled tough glumes tenaciously enclosing the seeds. After mechanical threshing, CS kernels exhibited a completely free-threshing phenotype (100%), while about 40% of S-6214 kernels were non-free-threshing. Both parents had tough rachises. However, under the same threshing conditions, a much higher percentage of nodes of the S-6214 spike rachis had broken, to produce wedge-type disarticulation (Table 1, Fig. 1). In general, all traits showed continuous variation and polygenic segregation patterns in F_2 progeny. Considerable transgressive segregation was observed in SPL and RCH. Besides the expected correlation between spike compactness (CPT), SPL, and number of spikelets per spike (SPN) (Table 2), CPT was positively correlated ($P < 0.001$) with FT and negatively correlated ($P < 0.001$) with RCH. Furthermore, SPL was negatively correlated with FT ($P < 0.001$), and SPN was negatively correlated with RCH ($P < 0.01$). FT and RCH were negatively correlated ($P < 0.001$). Consequently, plants with higher-density spikes tended to have higher FT and lower RCH.

Linkage map Out of 342 published simple sequence repeat (SSR) markers (Roeder et al., 1998; Pestsova et al., 2000; Gupta et al., 2002; Guyomarc'h et al., 2002; Somers et al., 2004; Sourdille et al., 2004; Song et al., 2005)

Table 1. Phenotypic analysis of quantitative spike traits in Chinese Spring, S-6214 and 117 F_2 individuals

Trait	Parents		F_2 Population			h^2
	Chinese Spring	S-6214	Max.	Min.	Mean	
Free-threshability (FT) (%)	100.00	59.62 ± 5.52	100.00	25.32	77.59 ± 16.14	0.94
Rachis fragility (RCH) (%)	2.52 ± 2.20	34.57 ± 7.92	49.36	4.17	23.89 ± 9.89	0.64
Spike length (SPL) (cm)	8.20 ± 0.5	11.60 ± 1.31	15.30	7.73	11.60 ± 1.54	0.59
Spikelet number per spike (SPN)	26.00 ± 1.73	18.33 ± 1.15	27.33	16.67	21.98 ± 2.21	0.56
Compactness (CPT)*	3.17 ± 0.11	1.59 ± 0.09	2.85	1.54	1.90 ± 0.22	0.81

* Compactness = spikelet number per spike/spike length.

Table 2. Pearson's correlation coefficients among domestication-related spike traits in 117 F_2 individuals

Trait	SPL	SPN	CPT	FT	RCH
SPL	–				
SPN	0.59***	–			
CPT	–0.68***	0.18*	–		
FT	–0.37***	–0.14ns	0.30***	–	
RCH	0.09ns	–0.26**	–0.31***	–0.32***	–

*, **, *** Significance at 0.05, 0.01 and 0.001 probability level, respectively.
ns: not significant.

screened for polymorphism between CS and S-6214, 229 SSRs representing 252 genetic loci were used to genotype 117 F_2 individuals. The linkage map spanned 2701.7 cM consisting of 253 loci across all 21 chromosomes (Fig. 2). Only 13% of the SSR loci were mapped as dominant markers and 6.32% showed significant segregation distortion. The genetic length of most chromosomes was comparable to that of the consensus SSR map (Somers et al., 2004) with the exception of chromosomes 5B and 6A, which were not well covered and contained linkage gaps. The mean distance between markers ranged from 5.6 cM on 4B and 6A to 16.3 cM on 6B, with the exception

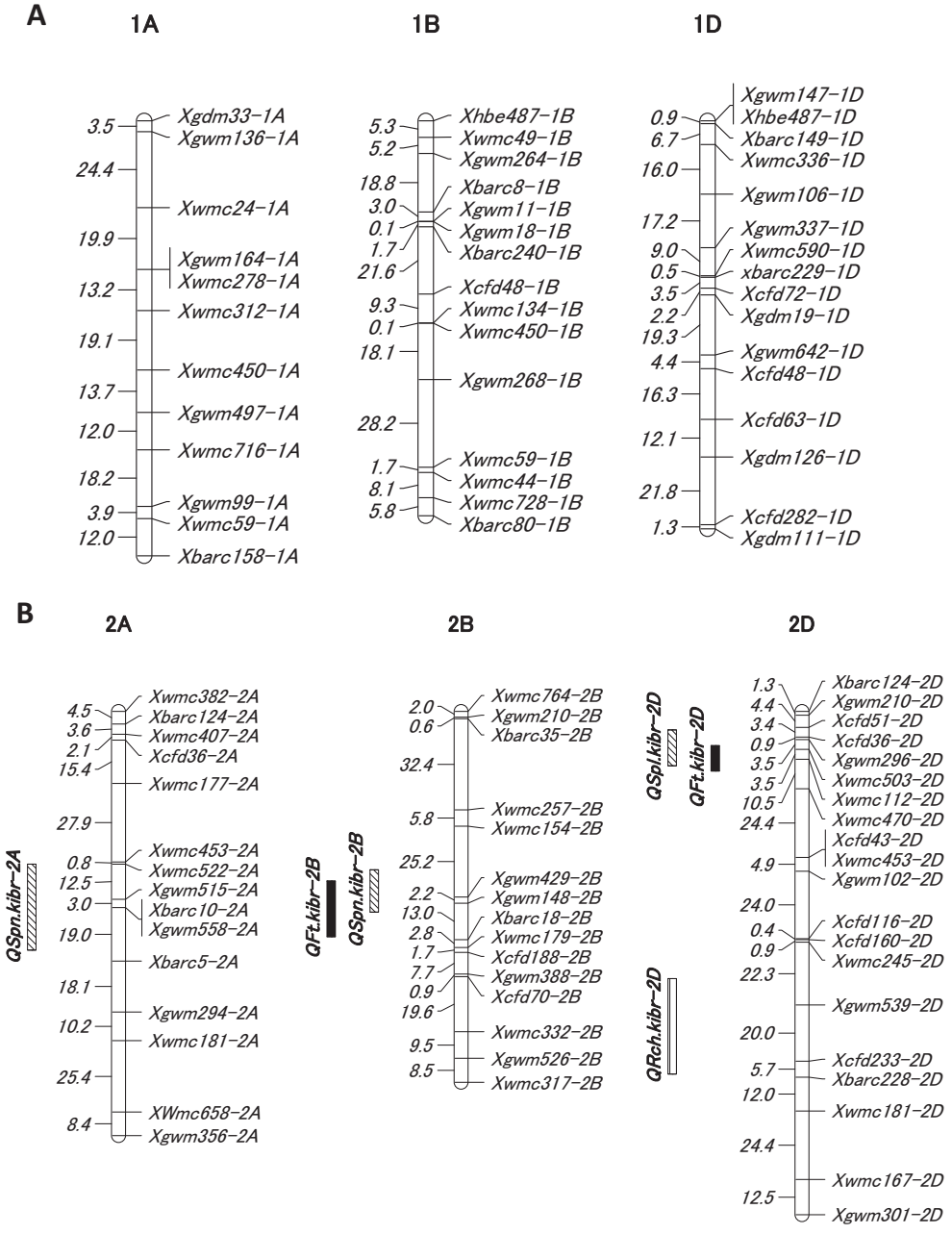

Fig. 2. Continued.

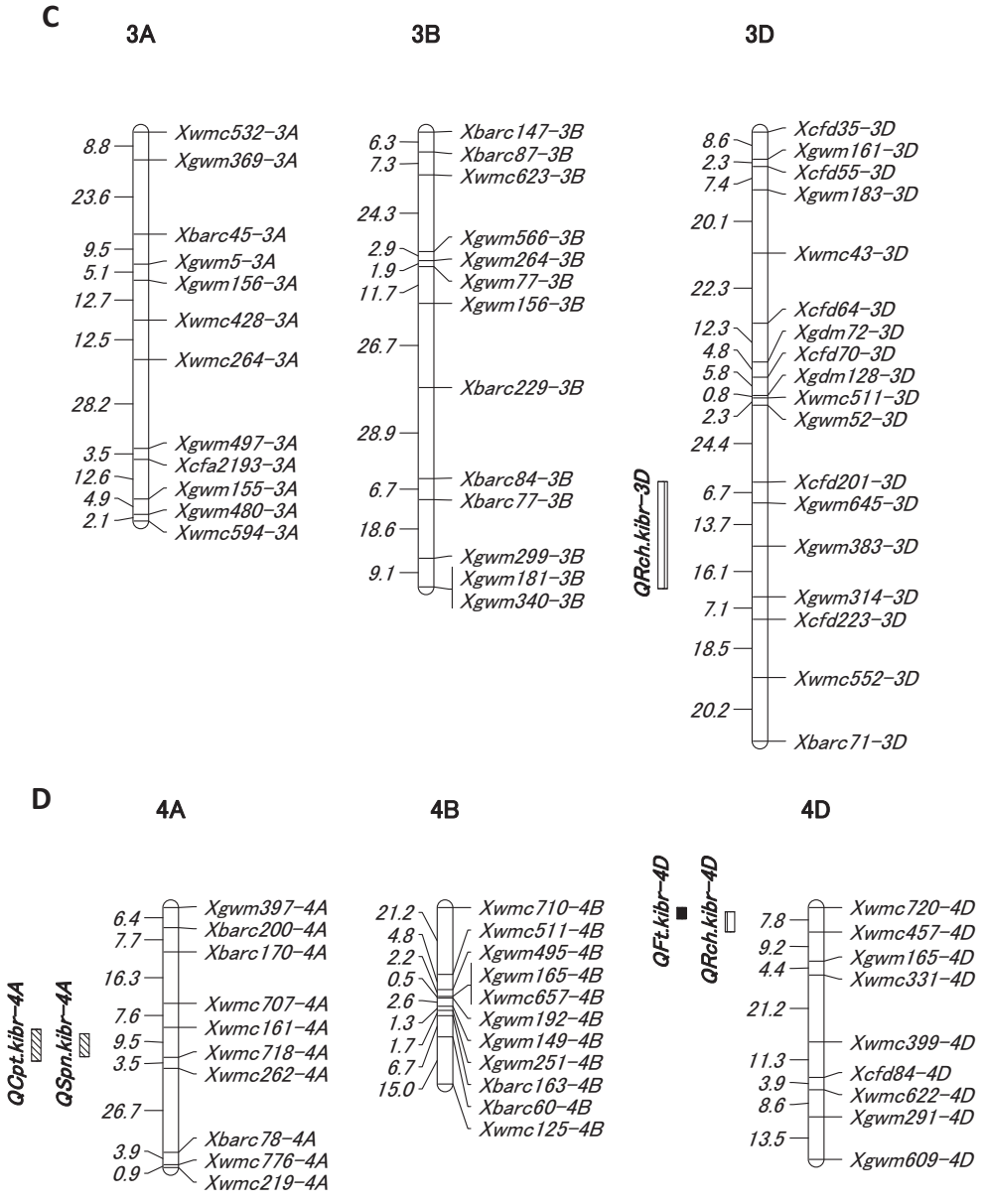

Fig. 2. Continued.

of low density on 7A (27.6 cM), and the overall interval mean was 11.61 cM. The A, B and D genome chromosomes had genetic lengths of 875.7 cM, 798.6 cM and 1027.4 cM with a mean distance between markers of 12.96 cM, 10.55 cM and 11.33 cM, respectively.

QTL analysis A total of 15 significant QTLs for domestication-related spike traits were detected (Table 3). The QTLs were distributed on eight chromosomes (Fig. 2).

Threshability (FT) The *Q* gene mainly controls free-threshability in domesticated polyploid wheats (Muramatsu, 1963). Although the location of the *Q* gene was mapped on 5AL, using the nucleotide polymorphism between CS and LDN upstream of the coding sequence of the *Q* genes (Supplementary Figs. S1 and S2), we found no QTLs corresponding to this region (Fig. 2E). On the other hand, four QTLs on 2BS, 2DS, 4D and 5DS (*QFt_kibr-2B*, *QFt_kibr-2D*, *QFt_kibr-4D*, *QFt_kibr-5D*) affected FT, respectively, accounting for 12, 22, 13, and 3% of the phenotypic variation (Table 3, Fig. 2). Increased FT was associated with the CS alleles at all these loci.

Rachis fragility The rachis of CS was not brittle after threshing. On the other hand, the rachis of S-6214 was fragile (Fig. 1). RCH in the F_2 population was affected by three QTLs (*QRch-2DL, QRch-3DL, QRch-4D*) accounting for 14, 16, and 35% of the phenotypic variation, respectively (Table 3, Fig. 2). Alleles from S-6214

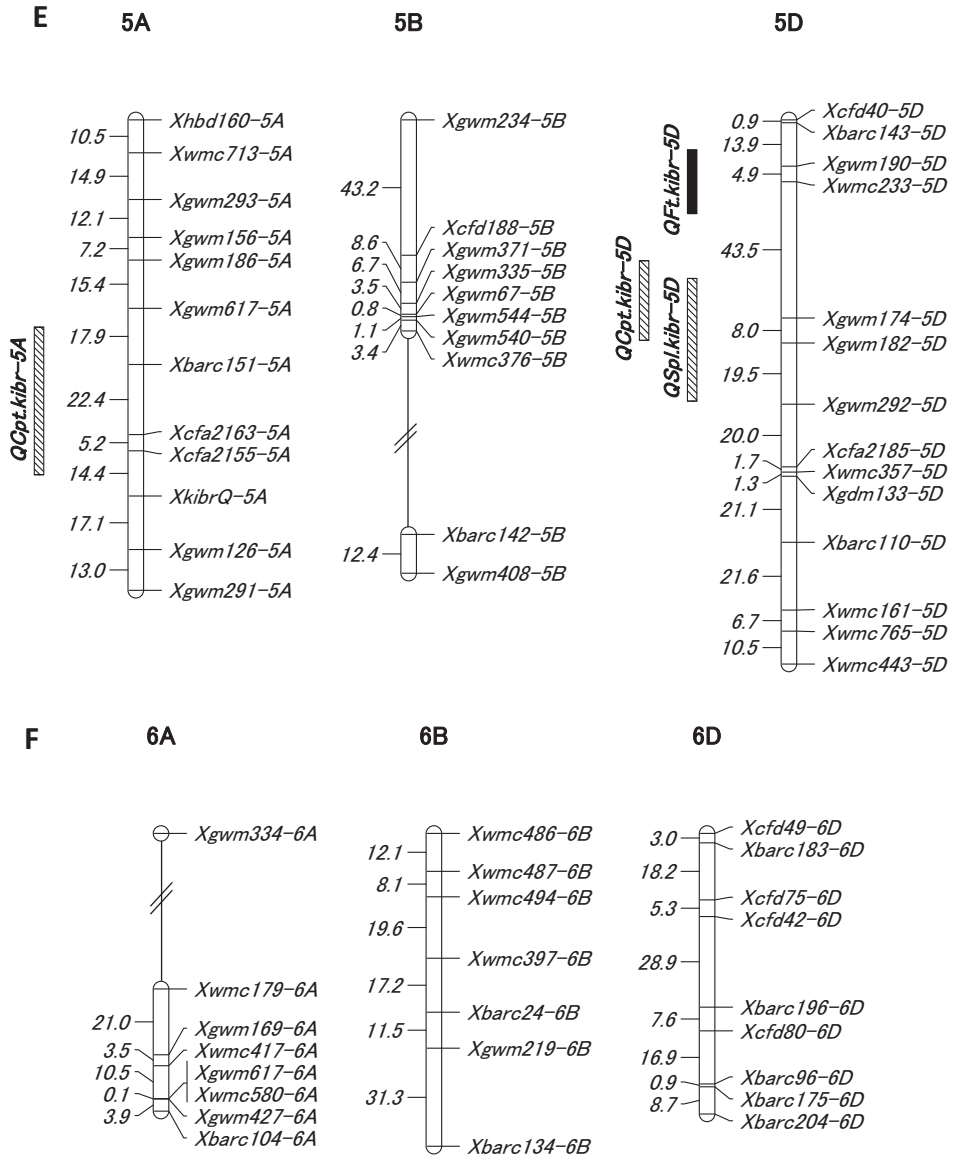

Fig. 2. Continued.

increased RCH at the QTLs on 2DL and 4D, while CS contributed the higher-value alleles at the QTL on 3DL.

Three rachis disarticulation types (i.e., wedge-type, barrel-type, and having both types) were found among the F_2 individuals with fragile rachises. To investigate the association of QTLs detected for RCH (*QRch*) with rachis disarticulation type, we examined the co-segregation of SSR markers closest to the *QRch* peaks (Dvorak et al., 2012) with rachis disarticulation type (Table 4). Plants showing both types of disarticulation were excluded from this test, so that 33 F_2 individuals for the wedge-type and 15 for the barrel-type were considered. While the parental alleles at relevant SSR loci on 2DL and 4D segregated independently of both disarticulation types, the barrel-type co-segregated with the CS allele at two SSRs, *Xgwm645* and *Xcfd201*, on 3DL with 1% level of significance. The wedge-type character, however, segregated independently from the parental alleles. This map position was different from those previously reported as associated with this character. *Br-D1* is linked to *Xgdm72-3D* (Watanabe et al., 2005). *Xgdm72-3D* was 38.1 cM away from *Xcfd201-3D*, which is the marker for this QTL (Fig. 2). While *Br-D2* was located in the 3L-0.81-1.00 BIN (Li and Gill, 2006), our QTL was in the 3L-0.22-0.81 BIN, distinct from the *Br-D2* region. The CS allele appears to promote the generation of barrel-type disarticulation at the 3DL locus. This gene is designated *Br-D3*. This is the first report to map the locus of a disarticulation-modifying gene in CS wheat.

Spike morphology Three QTLs associated with SPN were mapped to chromosomes 2AS, 2BS and 4AL (*QSpn-*

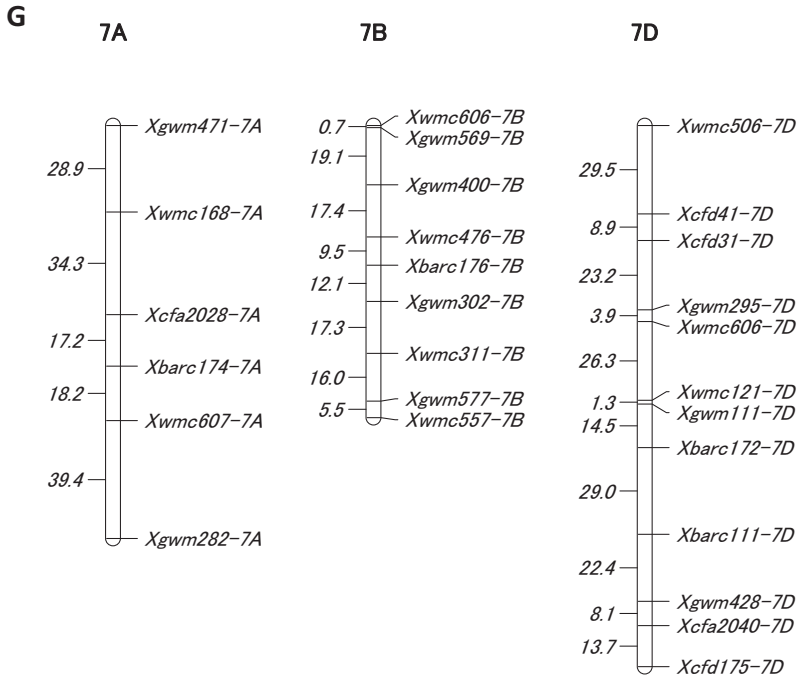

Fig. 2. Genetic linkage maps of whole chromosomes with 15 QTL peaks detected for domestication-related spike characters in hexaploid wheat. The numbers on the left of each chromosome represent genetic intervals in cM. Vertical bar: supported interval for each QTL; open bar: QTL for rachis fragility, black bar: QTL for free-threshability; stippled bar: QTL that affects spike compactness and its components, spike length and spikelet number.

Table 3. QTLs for domestication-related spike traits detected by composite interval mapping analysis

Trait	QTL	Marker interval[a]	Position[b]	Nearest marker	LOD[c]	A[d]	D[e]	D/A	R^2 (%)[f]
SPN	*QSpn.kibr-2AS*	*Xwmc522–Xbarc5*	71.8	*Xbarc10/Xgwm558*	3.6	0.70	0.30	0.43	5
	QSpn.kibr-2BS	*Xwmc154–Xbarc18*	64.8	*Xgwm429*	10.8	–1.20	–0.39	0.33	13
	QSpn.kibr-4AL	*Xwmc161–Xwmc718*	44.0	*Xwmc718*	11.6	1.39	0.48	0.35	17
SPL	*QSpl.kibr-2DS*	*Xcfd51–Xwmc470*	12.0	*Xwmc503*	4.2	–0.97	0.41	–0.42	18
	QSpl.kibr-5DL	*Xwmc233–Xgwm292*	65.2	*Xgwm174*	3.9	–0.94	0.54	–0.57	17
CPT	*QCpt.kibr-4AL*	*Xwmc161–Xwmc262*	44.0	*Xwmc718*	5.1	0.18	–0.07	–0.39	27
	QCpt.kibr-5AL	*Xgwm617–XkibrQ*	90.0	*Xcfa2163*	2.9	0.08	0.04	0.50	6
	QCpt.kibr-5DL	*Xwmc233–Xgwm182*	65.2	*Xgwm174*	5.5	0.15	–0.13	–0.87	23
FT	*QFt.kibr-2BS*	*Xwmc154–Xbarc18*	68.2	*Xgwm148*	2.8	7.99	–6.61	–0.83	12
	QFt.kibr-2DS	*Xgwm296–Xwmc470*	15.5	*Xwmc112*	4.7	10.87	–4.26	–0.39	22
	QFt.kibr-4D	*Xwmc720–Xwmc457*	0.0	*Xwmc720*	2.6	10.04	–3.19	–0.32	13
	QFt.kibr-5DS	*Xbarc143–Xgwm174*	16.8	*Xgwm190*	3.8	4.44	–10.80	–2.43	3
RCH	*QRch.kibr-2DL*	*Xwmc245–Xbarc228*	109.3	*Xgwm539*	3.4	–5.67	1.98	–0.35	14
	QRch.kibr-3DL	*Xcfd201–Xgwm314*	122.9	*Xgwm645*	3.3	5.89	–5.32	–0.90	16
	QRch.kibr-4D	*Xwmc720–Xwmc457*	6.0	*Xwmc457*	6.5	–12.34	–2.76	0.22	35

[a] 1-LOD support limit.
[b] Peak LOD score position.
[c] Peak LOD score.
[d] A = additive effect. A positive value indicates that the higher-value allele is from Chinese Spring alleles and a negative value indicates that the higher-value allele is from S-6214 alleles.
[e] D = dominant effect.
[f] R^2 = phenotypic variance explained.

2AS, *QSpn-2BS* and *QSpn-4AL*), explaining 5, 13 and 17% of the phenotypic variation, respectively (Table 3, Fig. 2). The CS parent contributed the higher-value alleles for the QTLs on chromosomes 2AS and 4AL, while S-6214 contributed the higher-value alleles for the QTL on 2BS. Two QTLs were identified for SPL on chromosomes 2DS and 5DL (*QSpl-2DS* and *QSpl-5DL*), accounting for 18 and 17% of the phenotypic variation, respectively (Table 3, Fig. 2). SPL was increased by the S-6214 alleles at both QTLs. CPT was affected by three QTLs on chromosomes 4AL, 5AL and 5DL (*QCpt-4AL*, *QCpt-5AL* and *QCpt-5DL*), explaining 27, 6 and 23% of the phenotypic variation, respectively (Table 3, Fig. 2). The increased CPT was contributed by CS alleles at these three loci.

Coincident QTLs were identified for CPT and SPN on 4AL, for SPN and FT on 2BS, for SPL and FT on 2DS, for RCH and FT on 4D, and for SPL and CPT on 5DL. These results indicate either that these QTLs represent genetic factors for pleiotropic effects or that tightly linked genes govern each character.

DISCUSSION

Five domestication-related spike traits (Table 1) of common wheat were mapped to eight chromosomes (Table 3, Fig. 2) using an F_2 population between CS wheat and a synthetic wheat produced by artificial crossing between LDN and wild goat grass. Since CS and LDN are cultivated types, both strains confer the genes as *QQbrbrtgtg* (e.g., Li and Gill, 2006). Supergene *Q* exhibits pleiotropic effects on domestic traits (Muramatsu, 1963) such as free-threshability, square head for spike morphology, rachis fragility, glume toughness and plant vigor. The *Q* gene in wheat was cloned as a homolog of *Arabidopsis APETALA2* (Simons et al., 2006). Although the *Q* genes of CS and LDN have identical coding sequences (Simons et al., 2006; Abdollahi et al., 2012), we found an insertion/deletion 1.5 kb upstream of the translation initiation site of the *Q* gene (Zhang et al., 2011; Supplementary Fig. S1). Using this polymorphism (Supplementary Fig. S2), we precisely mapped the *Q* gene on 5AL (Fig. 2E). As expected, no QTLs for free-threshability, square head for spike morphology, rachis fragility or glume toughness were found in this region, although the QTLs for glume tenacity and rachis fragility mapped around this region in the International Triticea Mapping Initiative (ITMI) population (Jantasuriyarat et al., 2004). On the other hand, the synthetic wheat S-6214 showed a non-domesticated phenotype, tough threshability, distinct spike morphology, and a more fragile rachis than CS due to addition of the non-domesticated genome of *Ae. tauschii* (Table 1, Fig. 1). From the observation of its phenotype in the field, *Ae. tauschii* is anticipated to confer *Br-DBr-DTgTgq-Dq-D* (Li and Gill, 2006; Abdollahi et al., 2012) plus additional genes.

In addition to the *Q* gene, threshability is governed by a partially dominant gene, *Tg-D1* (Kerber and Rowland, 1974; Simonetti et al., 1999). We found four QTLs for threshability (Table 3, Fig. 2). A QTL detected on 2DS coincided with one previously reported (Kerber and Rowland, 1974; Jantasuriyarat et al., 2004; Nalam et al., 2006; Sood et al., 2009; Dvorak et al., 2012), suggesting that this peak corresponds to *Tg-D1*. On the other hand, we detected another QTL peak on 2BS. The map position was apparently different from that of *Tg-B1* (Simonetti et al., 1999; Jantasuriyarat et al., 2004). This position was comparable to homoeoloci of *sog* (*soft glume*, Sood et al., 2009; Dvorak et al., 2012). Furthermore, we detected two more novel QTLs on 4D and 5DS. These genes should improve threshability.

Rachis fragility has long been believed to be a part of the spelt syndrome (*q* effects, Leighty and Boshnankian, 1921; MacKey, 1966). Since it was shown that fragile rachillae are formed under the control of the *Q* gene (Joppa and Cantrell, 1990; Chen, 2001), the gene(s) for rachis fragility or brittleness should be different from the *Q* gene. Our synthetic wheat, S-6214, showed partial rachis fragility (approximately 35%), while CS exhibited little rachis fragility (Table 1). Spikelets of parental S-6214 and CS displayed wedge-type disarticulation, but all three disarticulation types were found in the F_2 population, as in the case of semi-wild wheats in Tibet and Yunnan (Chen, 2001). Since *Ae. tauschii* showed full brittleness and barrel-type disarticulation, LDN gene(s) partially suppress rachis fragility and completely suppress barrel-type disarticulation in the synthetic hexaploid. On the other hand, CS gene(s) suppress rachis fragility. Segregation data from the F_2 progeny between CS and S-6214 suggest the existence of gene(s) to suppress gene action involved in rachis fragility, and in wedge-type and barrel-type disarticulation, in polyploid cultivated wheats. We detected three QTLs for rachis fragility after threshing, on 2DL, 3DL and 4D (Table 3, Fig. 2). Chen (2001) showed that several modifying genes control wedge-type or barrel-type disarticulation. These modifying genes for disarticulation type should be distinct from the genes for brittleness (Chen, 2001). We checked co-segregation of SSR markers with the disarticulation type. The allele of CS at the 3DL locus was tightly linked with that of the barrel-type disarticulation, while the other two loci showed no co-segregation with the disarticulation type gene (Table 4). Although genes for the barrel-type disarticulation (*Br-1* and *Br-2*) have been reported (Watanabe et al., 2005; Li and Gill, 2006), our gene, designated *Br-D3*, was at a different position from those. Although Tsunewaki et al. (1990) suggested the presence of *Br-D3* in CS, this is the first report on the mapping location of the barrel-type disarticulation type gene of CS.

Table 4. Co-segregation of SSR markers closest to the QTL peaks for rachis fragility and disarticulation types in 191 F_2 plants

Chromosome	Locus	Disarticulation type	No. of CS alleles	No. of S-6214 alleles	P value[a]
2DL	*Xgwm539*	barrel-type	3	4	0.705
		wedge-type	4	10	0.109
3DL	*Xgwm645*	barrel-type	12	0	0.001
		wedge-type	4	6	0.527
3DL	*Xcfd201*	barrel-type	10	1	0.007
		wedge-type	3	8	0.132
4D	*Xwmc457*	barrel-type	6	5	0.763
		wedge-type	11	13	0.683

[a] Probability of χ^2-value for fitting the CS allele vs. S-6214 allele ratio to the 1% ratio.

Eight QTLs related to spike morphology were detected in this study (Table 3, Fig. 2). Since a QTL on 4AL for spikelet number and spike compactness seemed to be located in the same region, and spike compactness is the spikelet number per unit spike length, the CS allele increased the spikelet number per spike in this background (Table 3). This location is comparable to that in the ITMI population. Simultaneously, loose spike compactness controlled by a QTL on 5DL should be attributable to the long spike length allele derived from S-6214. The QTL on 2BS affected spikelet number (Manickavelu et al., 2011), suggesting that this QTL region is consistent with the *Ppd-B1* gene (Worland, 1996; Sourdille et al., 2000; Li et al., 2002). Although its homoeotic QTL was found in the comparable region of 2AS, no QTL was detected on 2DS (Fig. 2). A QTL corresponding to the *Tg-D1* gene (Jantasuriyarat et al., 2004), which affects spike length and threshability, was detected on 2DS. On the other hand, a QTL located on 5AL of CS, which brought about spike compactness, was clearly different from the *Q* locus (Fig. 2, Jantasuriyarat et al., 2004; Ma et al., 2007; Kosuge et al., 2012). Durum wheat seems not to carry this gene (Jantasuriyarat et al., 2004).

While certain QTLs that control spike morphology were confirmed (on 2AS, 2BS, 2DS, 4AL and 5AL), a new QTL for spike length located on 5DL was found. Although spike morphology is governed by a number of genes, identification of each gene by QTL analysis using characteristic trait combinations provides new information to pyramidize useful genes in elite cultivars.

This work was partly supported by Grants-in-Aid for scientific research in the priority area "Comparative Genomics" from the Ministry of Education, Culture, Sports, Science and Technology of Japan. This is contribution No. 1018 from the Kihara Institute for Biological Research, Yokohama City University.

REFERENCES

Abdollahi, P., Kamiya, Y., Kawaura, K., and Ogihara, Y. (2012) Overexpression of *Q*/*q*-related homoeoalleles of hexaploid wheat reveals distinct recovery of flower transformation in the *apetala2* mutant of *Arabidopsis*. Plant Biotech. **29**, 245–252.

Chen, Q-F. (2001) Inheritance of disarticulation derived from some hexaploid brittle rachis wheat. Genet. Resour. Crop Evol. **48**, 21–25.

Chen, Q-F., Yen, C., and Yang, J-L. (1998) Chromosome location of the gene for brittle rachis in the Tibetan weedrace of common wheat. Genet. Resour. Crop Evol. **45**, 407–410.

Dvorak, J., Deal, K. R., Luo, M-C., You, F. M., Borstel, K. V., and Dehghani, H. (2012) The origin of spelt and free-threshing hexaploid wheat. J. Hered. **103**, 426–441.

Gupta, K., Balyan, S., Edwards, J., Issac, P., Korzun, V., Röder, M., Gautier, M. F., Joudrier, P., Schlatter, R., Dubcovsky, J., et al. (2002) Genetic mapping of 66 new microsatellite (SSR) loci in bread wheat. Theor. Appl. Genet. **105**, 413–422.

Guyomarc'h, H., Sourdille, P., Charmet, G., Edwards, J., and Bernard, M. (2002) Characterization of polymorphic microsatellite markers for *Aegilops tauschii* and transferability to the D-genome of bread wheat. Theor. Appl. Genet. **104**, 1164–1172.

Jantasuriyarat, C., Vales, M. I., Watson, C. J. W., and Riera-Lizarazu, O. (2004) Identification and mapping of genetic loci affecting the free-threshing habit and spike compactness in wheat (*Triticum aestivum* L.). Theor. Appl. Genet. **108**, 261–273.

Joppa, L. R., and Cantrell, G. R. (1990) Chromosomal location of genes for grain protein content of wild tetraploid wheat. Crop Sci. **30**, 1059–1064.

Kerber, E. R., and Dyck, P. L. (1969) Inheritance in hexaploid wheat of leaf rust resistance and other characters derived from *Aegilops squarrosa*. Can. J. Genet. Cytol. **11**, 639–647.

Kerber, E. R., and Rowland, G. G. (1974) Origin of the free threshing character in hexaploid wheat. Can. J. Genet. Cytol. **16**, 145–154.

Kihara, H. (1944) Discovery of the DD-analyser, one of the ancestors of *Triticum vulgare*. Agric. Hortic. **19**, 889–890.

Kimber, G., and Feldman, M. (1987) Wild Wheat: An Introduction. University of Missouri-Columbia, Columbia, USA.

Kosambi, D. (1943) The estimation of map distances from recombination values. Ann. Eugen. **12**, 172–175.

Kosuge, A., Watanabe, N., Melnik, V. M., Laikova, L. I., and Goncharov, N. P. (2012) New sources of compact spike morphology determined by the genes on chromosome 5A in hexaploid wheat. Genet. Resour. Crop Evol. **59**, 1115–1124.

Lander, E. S., Green, P., Abrahamson, J., Barlow, A., Daly, M. J., Lincoln, S. E., and Newburg, L. (1987) MAPMAKER: an interactive computer package for constructing primary genetic linkage maps of experimental and natural populations. Genomics **1**, 174–181.

Leighty, C. E., and Boshnankian, S. (1921) Genetic behaviour of the spelt form in crosses between *Triticum spelta* and *Triticum aestivum*. J. Agric. Res. **7**, 335–364.

Li, W. L., Nelson, J. C., Chu, C. Y., Shi, L. H., Huang, S. H., and Liu, D. J. (2002) Chromosomal locations and genetic relationships of tiller and spike characters in wheat. Euphytica **125**, 357–366.

Li, W., and Gill, B. S. (2006) Multiple genetic pathways for seed shattering in the grasses. Funct. Integr. Genomics **6**, 300–

309.

Ma, Z., Zhao, D., Zhang, C., Zhang, Z., Xue, S., Lin, F., Kong, Z., Tian, D., and Luo, Q. (2007) Molecular genetic analysis of five spike-related traits in wheat using RIL and immortalized F2 populations. Mol. Gen. Genomics **277**, 31–42.

MacKey, J. (1966) Species relationship in *Triticum*. Proc. 2nd Int. Wheat Genet. Symp. (Hereditas Suppl) **2**, 237–276.

Manickavelu, A., Kawaura, K., Imamura, H., Mori, M., and Ogihara, Y. (2011) Molecular mapping of quantitative trait loci for domestication traits and β-glucan content in a wheat recombinant inbred line population. Euphytica **177**, 179–190.

McFadden, E. S., and Sears, E. R. (1946) The origin of *Triticum spelta* and its free-threshing hexaploid relatives. J. Hered. **37**, 81–89.

Muramatsu, M. (1963) Dosage effect of the spelt gene *q* of hexaploid wheat. Genetics **48**, 469–482.

Nalam, V. J., Vales, M. I., Watson, C. J. W., Kianian, S. F., and Riera-Lizarazu, O. (2006) Map-based analysis of genes affecting the brittle rachis character in tetraploid wheat (*Triticum turgidum* L.). Theor. Appl. Genet. **112**, 373–381.

Pestsova, E., Ganal, M. W., and Roeder, M. S. (2000) Isolation and mapping of microsatellite markers specific for the D genome of bread wheat. Genome **43**, 689–697.

Roeder, M. S., Korzun, V., Wandehake, K., Plaschke, J., Tixier, M. H., Leroy, P., and Ganal, M. W. (1998) A microsatellite map of wheat. Genetics **149**, 2007–2023.

Saghai-Maroof, M. A., Soliman, K. M., Jorgensen, A. R., and Allard, R. W. (1984) Ribosomal DNA spacer length polymorphism in barley: Mendelian inheritance, chromosomal location and population dynamics. Proc. Natl. Acad. Sci. USA **81**, 8014–8018.

Simonetti, M. C., Bellomo, M. P., Laghetti, G., Perrino, P., Simeone, R., and Blanco, A. (1999) Quantitative trait loci influencing free-threshing habit in tetraploid wheats. Genet. Resour. Crop Evol. **46**, 267–271.

Simons, K. J., Fellers, J. P., Trick, H. N., Zhang, Z., Tai, Y-S., Gill, B. S., and Faris, J. D. (2006) Molecular characterization of the major wheat domestication gene *Q*. Genetics **172**, 547–555.

Somers, D. J., Issac, P., and Edwards, K. (2004) A high-density microsatellite consensus map for bread wheat (*Triticum aestivum* L.). Theor. Appl. Genet. **109**, 1105–1114.

Song, Q. J., Shi, J. R., Singh, S., Fickus, E. W., Costa, J. M., Lewis, J., Gill, B. S., Ward, R., and Cregan, P. B. (2005) Development and mapping of microsatellite (SSR) markers in wheat. Theor. Appl. Genet. **110**, 550–560.

Sood, S., Kuraparthy, V., Bai, G., and Gill, B. S. (2009) The major threshability genes soft glume (*sog*) and tenacious glume (*Tg*), of diploid and polyploid wheat, trace their origin to independent mutations at non-orthologous loci. Theor. Appl. Genet. **119**, 341–351.

Sourdille, P., Tixier, M. H., Charmet, G., Gay, G., Cadalen, T., Bernard, S., and Bernard, M. (2000) Location of genes involved in ear compactness in wheat (*Triticum aestivum*) by means of molecular markers. Mol. Breed. **6**, 247–255.

Sourdille, P., Singh, S., Cadalen, T., Brown-Guedira, G. L., Gay, G., Qi, L., Gill, B. S., Dufour, P., Murigneux, A., and Bernard, M. (2004) Microsatellite-based deletion bin system for the establishment of genetic-physical map relationships in wheat (*Triticum aestivum* L.). Funct. Integr. Genomics **4**, 12–25.

Tsunewaki, K., Yamada, S., and Mori, N. (1990) Genetical studies on a Tibetan semi-wild wheat, *Triticum aestivum* ssp. *tibetanum*. Jpn. J. Genet. **65**, 353–365.

Voorrips, R. E. (2002) MapChart: software for the graphical presentation of linkage maps and QTLs. J. Hered. **93**, 77–78.

Wang, S., Basten, C. J., and Zeng, Z. B. (2005) Windows QTL Cartographer v2.5. Program in Statistical Genetics, North Carolina State University.

Watanabe, N., Sugiyama, K., Yamagishi, Y., and Sakata, Y. (2002) Comparative telosomic mapping of homoeologous genes for brittle rachis in tetraploid and hexaploid wheats. Hereditas **137**, 180–185.

Watanabe, N., Takesada, N., Shibata, Y., and Ban, T. (2005) Genetic mapping of the genes for glaucous leaf and tough rachis in *Aegilops tauschii*, the D-genome progenitor of wheat. Euphytica **144**, 119–123.

Watanabe, N., Fujii, Y., Kato, N., Ban, T., and Martinek, P. (2006) Microsatellite mapping of the genes for brittle rachis on homoeologous group 3 chromosomes in tetraploid and hexaploid wheats. J. Appl. Genet. **47**, 93–98.

Worland, A. J. (1996) The influence of flowering time genes on environmental adaptability in European wheats. Euphytica **89**, 49–57.

Zeng, Z. (1993) Theoretical basis for separation of multiple linked gene effects in mapping quantitative trait loci. Proc. Natl. Acad. Sci. USA **90**, 10972–10976.

Zeng, Z. (1994) Precision mapping of quantitative trait loci. Genetics **136**, 1457–1468.

Zhang, Z., Belcram, H., Gornicki, P., Charles, M., Just, J., Huneau, C., Magdelenat, G., Couloux, A., Samain, S., Gille, B. S., et al. (2011) Duplication and partitioning in evolution and function of homoeologous *Q* loci governing domestication characters in polyploid wheat. Proc. Natl. Acad. Sci. USA **108**, 18737–18742.